Techniques in X-ray Astronomy

2. Imaging Detectors

Kulinder Pal Singh

Kulinder Pal Singh is in the Department of Astronomy and Astrophysics of the Tata Institute of Fundamental Research, Mumbai. His primary fields of research are X-ray studies of hot plasmas in stars, supernova remnants, galaxies, intergalactic medium in clusters of galaxies, active galactic nuclei, cataclysmic variables and X-ray binaries. He is leading the development of a soft X-ray imaging telescope for the ASTROSAT mission to be launched by India in 2007-2008.

The excellent X-ray images produced by X-ray telescopes require the use of detectors with imaging capability at the focal plane of the telescopes. In this concluding part of the article on experimental techniques in X-ray astronomy, I describe many X-ray detectors that have been used over the years. These can broadly be classified into two physical types: non-dispersive and dispersive. Traditionally the simple non-dispersive types have been used extensively in X-ray astronomy. The advancement of solid state technologies, cryogenics, and the quality of X-ray imaging has led to many new detectors of both types. Both the traditional and the new types of detectors are described briefly here with emphasis on principles and some technical details.

Introduction

A variety of focal plane instruments have been built for recording the X-ray images produced using grazing incidence X-ray telescopes. These include the Position Sensitive Proportional Counter (PSPC), Micro Channel Plate (MCP), Charge Coupled Device (CCD), and micro-calorimeter. Except for the micro-calorimeters, the energy resolution of these detectors is generally low ($E/\Delta E$ = 1-5 for PSPC, 10-60 for CCD, 200-1000 for micro-calorimeter) when compared to that prevalent in optical astronomy. The combination of a telescope with a CCD provides a powerful tool for energy dependent imaging that can isolate regions of continuum emission from that of line emission from various ions in a hot X-ray emitting gas as in the case of supernova remnants and clusters of galaxies. In addition, wavelength dispersive instruments like transmission or reflection gratings have been built and flown to provide high resolution X-

[1] Part 1. Imaging Telescopes, *Resonance*, Vol.10, No.5, pp.15-23, 2005.

Keywords
X-ray astronomy, imaging detectors.

ray spectroscopy with E/ΔE about 1000.

Non-dispersive X-ray Detectors

Proportional counters have been the most extensively used non-dispersive detectors in X-ray astronomy for typical X-ray photon energies in the range of 0.1 to 30 keV. X-rays are detected by photo-ionization of a gas mixture contained in a windowed gas cell, subdivided into a number of low- and high-electric field regions by an arrangement of electrodes. X-rays interact with gas atoms via the photoelectric effect, with the immediate release of a primary photoelectron, followed by a cascade of Auger electrons and/or fluorescent photons. Basically, once a gas atom is ionized by photons, the free electron is attracted to the positive anode wire at the center of the cell. This electron then ionizes more atoms through collisions. Subsequent electrons may recombine with ionized atoms, emitting a photon, which photo-ionizes more atoms. Hence there is a cascade of electrons to the anode, which results in an electrical impulse at the anode wire. The signals induced on these electrodes by the motions of electrons and ions in the counting gas mixture contain information on the energies, arrival times, and interaction positions of the photons transmitted by the window. The absorption cross-section of the gas determines the energy sensitivity of the detector, with the greatest sensitivity lying at energies just above the absorption edges. Photons deposit all of their energy within a short distance in the detector, so that only one cell is activated. A charged particle ionizes the gas through collisions, hence leaving a trail of ionized particles through more than one cell. In addition to rejecting charged particles by the number of cells they activate, such signals can also be rejected because the shape of their analog pulse differs from those of X-rays. For a satellite in a high-Earth orbit (> 1000 km) the environment is influenced by solar cycle and the isotropic interplanetary cosmic ray flux. In a low-Earth orbit (500 to 600 km) the influences are primarily from cosmic rays, albedo electrons, Compton scattered photons, trapped electrons, and induced radioactivity, leading to a background heavily dependent

In a low-Earth orbit (500 to 600 km) the influences are primarily from cosmic rays, albedo electrons, Compton scattered photons, trapped electrons, and induced radioactivity, leading to a background heavily dependent on satellite latitude.

on satellite latitude. In a low-Earth orbit, the raw background count rates can be an order of magnitude less than in interplanetary space. Large area detectors of this type are usually employed in low-Earth orbits and have been the workhorses for X-ray astronomy, particularly in the energy range where focusing of X-rays is difficult. However, making very large systems of this type leads to a very heavy system and very quickly gets background dominated, thus affecting the sensitivity that can be achieved.

PSPCs have been used at the focal plane of the X-ray telescopes (*Einstein Observatory, ROSAT*). Position sensitivity is obtained by electronic position encoding of the charge cloud either digitally or in an analog fashion. A digital encoder associates a preamplifier and counting circuit with each pixel, or resolution element, of the field. An analog system estimates event coordinates from the properties of voltage waveforms at different output electrodes. Digital schemes are capable of handling higher count rates, but are more complex systems. In X-ray astronomy, where count rates are typically low and system simplicity is a good thing, the analog readout, in which it is the centeroid of the induced charge distribution that is encoded, is more common.

High Resolution X-ray Cameras Consisting of MCPs have been flown on the *Einstein Observatory, ROSAT and CXO*. These typically consist of 2 MCPs (*Figure* 1 (left)). In CXO, each MCP is a cluster of tiny lead-oxide glass tubes with a special coating

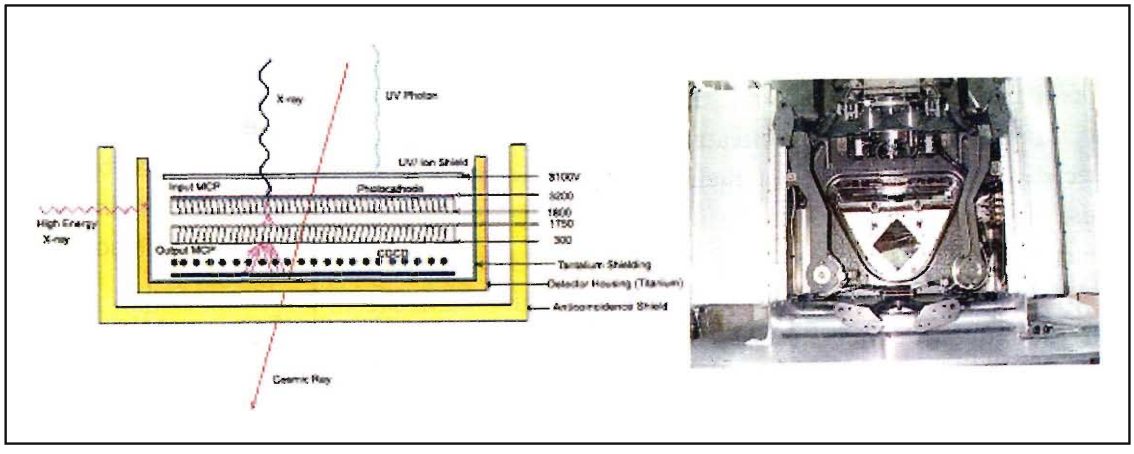

Figure 1. X-ray imaging camera using micro-channel plates (schematic on the left) and actual camera on CXO (right). Each MCP is a postcard-sized (10 cm²) cluster of 69 million tiny lead-oxide glass tubes that are about 10 μm in diameter and 1.2mm long.

that causes electrons to be released when the X-rays hit the tubes. These electrons are accelerated down the tube by a high voltage, releasing more electrons as they bounce off the sides of the tube. By the time they leave the end of the tube, they have created a cloud of tens of million electrons. A crossed grid of wires detects this electronic signal and allows the position of the original X-ray photon to be determined with high precision.

In a CCD used commonly in digital cameras, visible light photon releases only one electron-hole pair, and consequently many photons must be collected in each pixel for a measurable signal to be produced. Therefore, at visible wavelengths CCDs are used as integrating detectors, and typically the astronomical image exposures are several minutes long. However, a single X-ray photon has sufficient energy to form multiple electron-hole pairs through the process of secondary ionization by the primary photoelectron. An average of one electron-hole pair is liberated for each 3.65 eV of photon energy absorbed. The charge liberated by a single X-ray photon (about 100-1000 electrons) is easily detectable if the amplifier noise is low enough. Therefore, at X-ray energies, CCDs can be used as photon counting detectors, with the measured signal proportional to the photon energies. However, very special high purity and high resistivity Si is required for large depletion depths (about 40 μm) to stop 8-10 keV X-ray photons. Consequently, X-ray CCDs are not commercially available.

A single X-ray photon has sufficient energy to form multiple electron-hole pairs through the process of secondary ionization by the primary photoelectron.

In a CCD chip, incident X-ray photons are converted into electronic signals that record the location of the event and its energy. Spatial resolution obtainable with a CCD is limited by the physical dimensions of the discrete charge collecting locations (called picture elements or pixels). These pixels are typically 20-40 μm square with essentially no spacing or dead area between them. The number of pixels varies from 500 to 1000. CCDs used in X-ray astronomy are of frame-store type generally used in TV imaging. An array of vertical electrodes is formed over the silicon surface and horizontal charge transfer columns are defined by implanted channel stop regions in the wafer

CCDs used in X-ray astronomy are of frame-store type generally used in TV imaging.

surface. These orthogonally aligned elements are produced by conventional MOS fabrication procedures. Application of suitable bias voltages to the electrodes produces a matrix of potential wells that define the CCD picture elements. Each pixel of the CCD stores the signal generated in it by an incident X-ray for a period of a few seconds. The electrodes are generally arranged in two groups; one group is fabricated over the top half of the array, and a second group over the bottom half. This latter half is shielded from X-rays, and is used to store successive image data frames previously collected in the 'image' section. This eliminates the requirement for a mechanical shutter to shield the array during readout, since the data transfer from image to store section is accomplished in a few tens of milliseconds taken to read out the data in the array. In most applications, the incident X-ray flux will be low enough that only a single X-ray will be detected for every 100 or more pixels sampled. When this is true, the electronic signal is related to the energy of the X-ray with reasonably high accuracy ($E/\Delta E = 50$), and the instrument simultaneously functions as a high spatial resolution detector and moderate spectral resolution spectrometer. For higher flux sources, either special operating modes are required, or the analysis must allow for the possibility of multiple photons per pixel ('pile-up').

As a CCD does not produce a prompt signal when it is struck by an X-ray, but instead must wait for the CCD to be read out through a command, the timing resolution is limited by the time between successive readouts. This results in a typical time resolution on photon arrival times of a few seconds. If better time resolution is required, however, CCDs can be operated in several special modes that reduce the time between readouts but also drastically reduce the field of view. Complications are charge transfer efficiency, cooling to about –60 to –100 degrees C, radiation damage in orbit. X-ray CCD cameras were first flown on ASCA, and are now flying at the focal planes of *Chandra*, XMM-*Newton*, and *SWIFT* observatories (see *Figure* 2).

X-ray calorimeters measure energy of the incident X-ray photon by determining temperature rise of the absorbing material.

X-ray Calorimeters measure energy of the incident X-ray

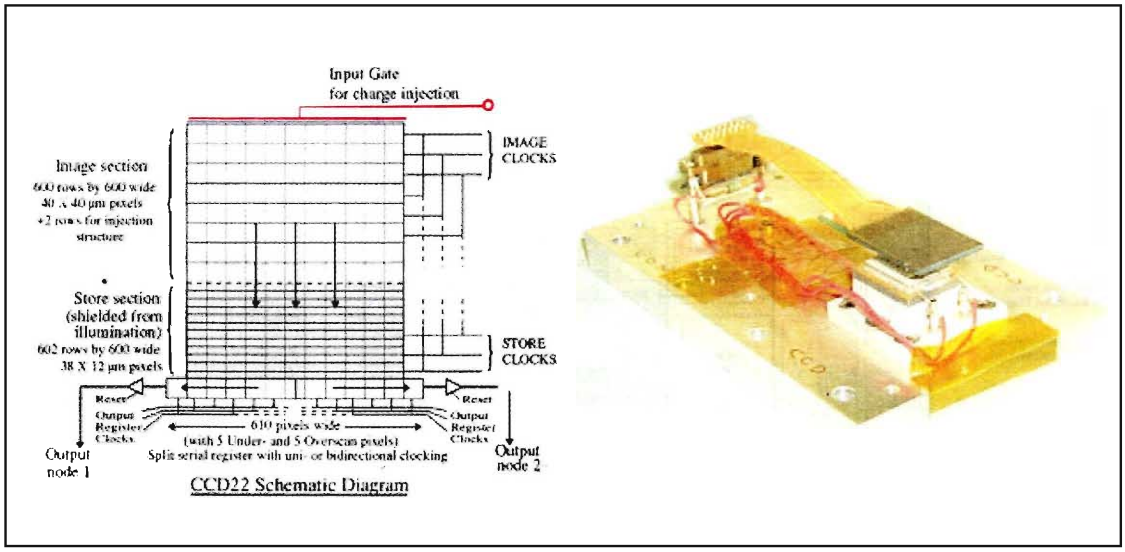

Figure 2. X-ray CCD chip (SWIFT) showing image store regions (left) and mounted on a thermo-electric cooler (right).

photon by determining temperature rise of the absorbing material, which has to be sufficiently opaque to X-rays. Energy resolution of the calorimeter is higher for lower heat capacity of the absorber. A calorimeter array has been made for flying on *ASTRO-E2* (see *Figure* 3). On each pixel, HgTe absorber is attached on the monolithic silicon substrate in which a thermistor is ion-implanted. The thermistor changes its resistance with the temperature in the range of 10-50 mega-ohms, and as a result the temperature increase is detected as a change of the voltage across it. Signal from each thermistor is picked up by a JFET and sent to the Calorimeter Analogue Processor (CAP) individually. The detector assembly will have to be kept at 65 milliKelvin within accuracy of tens of micro-Kelvins to operate at the maximum performance. The rise time of the temperature is a few millisecond, and the total recovery time is about 80 ms, which determines the maximum counting rate of the observable sources. Beneath the calorimeter array, a silicon PIN anti-coincidence detector is put in order to detect background particles that may penetrate the calorimeter array. X-rays that are simultaneously detected with the anti-coincidence detector are flagged and may be rejected in later data analysis. Such calorimeters will provide very high resolution ($E/\Delta E$ = 40 to 1000) spectra (comparable to that obtained with the gratings below)

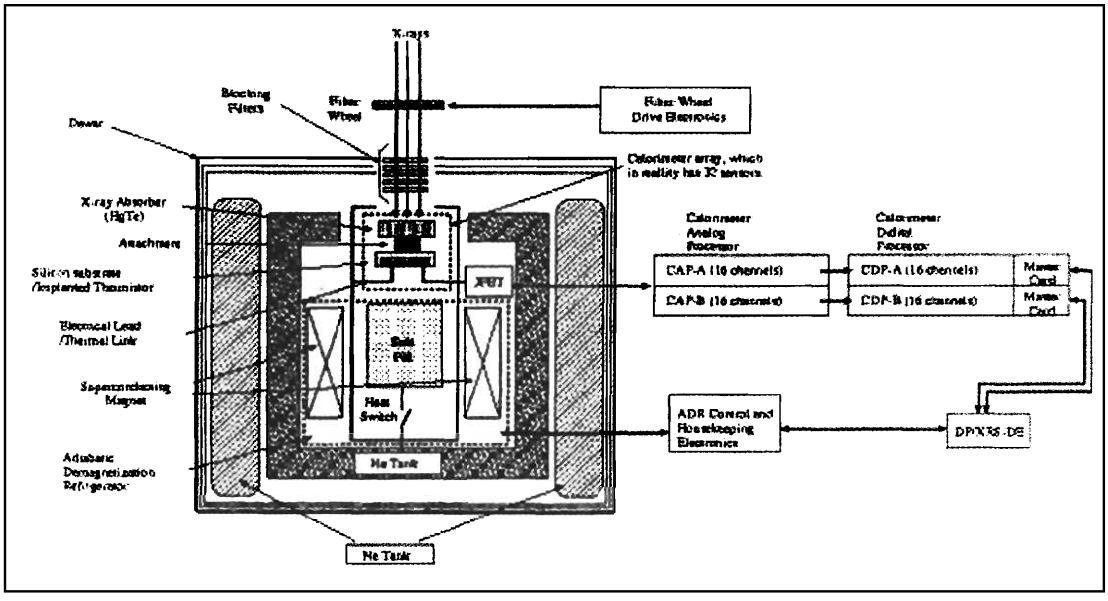

Figure 3. X-ray micro-calorimeter, the Adiabatic Demagnetization Refrigerator, the liquid helium tank and the solid neon tank to be flown on ASTRO-E2 in 2005. The calorimeter array, cooled to 65 mK, consists of 32 active pixels each of size 625 x 625 μm, covering roughly 3'x3' area on the sky. CAP provides power to the detector and amplifies the signals by a factor of 20,000. CAP has 32 channels, each of which handles data from a single calorimeter pixel. The helium tank filled with 25 litres of liquid helium whose temperature is about 1.5 K. It is surrounded by the neon tank that is filled with 100 litre solid neon at a temperature of about 17 K. The time required for all the solid neon to completely melt determines the lifetime of the instrument (about 2 years).

but with a much higher efficiency than that of the gratings and over a very wide energy band of 0.3 to 10 keV.

Most of the detectors described above are useful only for soft X-rays (E <10 keV). Solid state detectors made from Cadmium Telluride with band gap energy of 1.5 eV, high atomic number (Z_{Cd}=48 and Z_{Te}=52) can detect photons with energy up to 100 keV even for a thickness of 0.5mm. However, the energy resolution of such a device is poor due to hole-trapping. An alloy of CdTe and Zn (CdZnTe) with a higher resistivity (10^{11} Ωcm compared to 4×10^9 Ωcm for CdTe) has a better energy resolution. A large area (5200 cm^2) CdZnTe detector with a coded aperture mask is currently flying on SWIFT observatory for the detection of γ-ray bursts. The coded aperture made of Pb tiles

helps in locating the γ-ray burst positions in the sky to an accuracy of 4 arcmins over a wide field of 1.5 steradians. The development of hard X-ray telescopes will require imaging detectors for hard X-rays. Pixellated CdZnTe detectors with a grid structure have been developed for imaging hard X-rays, and can be used for medical imaging as well as hard X-ray astronomy.

Dispersive X-ray Detectors

BRAGG Crystal X-ray Spectrometer

A dispersive X-ray spectrometer based on the principle of Bragg Diffraction ($2d \sin\theta = \lambda = h$) was flown on the *Einstein Observatory*. Crystals were mounted on toroidal geometry to intercept the X-ray beam at nearly constant Bragg angle. The arrangement used in the *Einstein Observatory* is shown in *Figure* 4. Crystals were chosen to cover the energy range of the X-ray telescope and astronomically important X-ray wavelengths for diagnostics of hot plasmas using line emission from highly ionized atoms of N, O, Ne, Si and S that occur abundantly in stars and galaxies. These include the 1s-2p (Lyα) and 1s-3p (Lyβ) transitions in the hydrogenic ions N VII, O VIII, Ne X, Si XIV, and S XVI; the $1s^2$-1s2p (^1P) (resonance), $1s^2$-1s2p (^3P) (intercombination), $1s^2$-1s2s (^3S) (forbidden) transitions in the helium-like ions N VI, O VII, Ne IX, Mg XI, Si XIII and S XV;

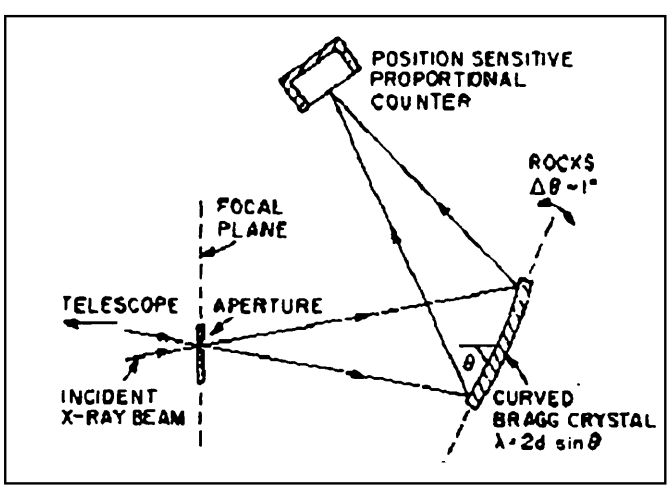

Figure 4. A schematic of the Bragg Crystal Spectrometer flown on the Einstein Observatory in 1978. Six different crystals were used to cover line features in the energy range from 0.42 - 2.6 keV. Crystals were pentaerythritol (PET, 2d=8.7 Å), ammonium dihydrogen phosphate (ADP, 2d=10.6 Å), thalium acid phthalate (TAP, 2d=25.8 Å), rubidium acid phthalate (RAP, 2d=26.1 Å), lead laurate (PBL, 2d=70 Å), lead stearate (PBSt, 2d=100 Å).

the fluorescence lines Si I Kα and Fe I Kα, and absorption edges etc. Although these spectrometers provide extremely high resolution (E/ΔE = 100 to 1000), their bandwidth is very narrow. In a typical observation, a small segment (20-80 eV) of spectrum could be obtained centered on a specific spectral feature by stepping the orientation of the selected crystal.

Reflection and Transmission Gratings

When a reflection or a transmission grating is introduced into the light path between the X-ray mirrors and the focal plane detector, the image of a source becomes dispersed and a very high spectral resolution becomes possible over a much wider energy range than obtainable with the Crystal Spectrometers. Reflection gratings have been built and are currently in use in the *XMM-Newton*, providing high resolution (E/ΔE = 200 to 800) X-ray spectroscopy over the energy range 0.35-2.5 keV (5-35 Å). The gratings are mounted at precise angles to the incoming radiation in order to get the best resolution on the camera. About half of the light incident on the array grazes off the plates that act like a prism. This disperses the light into its component wavelengths and focuses it onto the camera offset to the side. The other half of the light continues directly toward the imaging camera at the telescope focus. The gratings, detector strip, and the imaging camera are all aligned around a Rowland Circle (*Figure* 5). This geometry is ideal because it eliminates spherical aberrations that would contaminate the detector images. The diffracted light is recorded by a camera that takes a picture of the spectrum. The spectrum appears as a line image across the width of the detectors.

The line emission can provide a detailed diagnostics – density, temperature, composition, state of equilibrium of the hot plasma emission from stars and other X-ray sources (clusters of galaxies and supernova remnants) containing hot ionized gas.

Examples of X-ray spectra taken with the *XMM-Newton* Reflection Grating Spectrometer (RGS) showing a range of continua and line emission are displayed in *Figure* 6. Four late-type stars with very different coronal temperatures during quiescence shown from top to bottom are: (a) YY Men, a late type giant with a maximum temperature of >30 MK; (b) HR 1099, a binary consisting of two late type sub-giant stars with a maximum

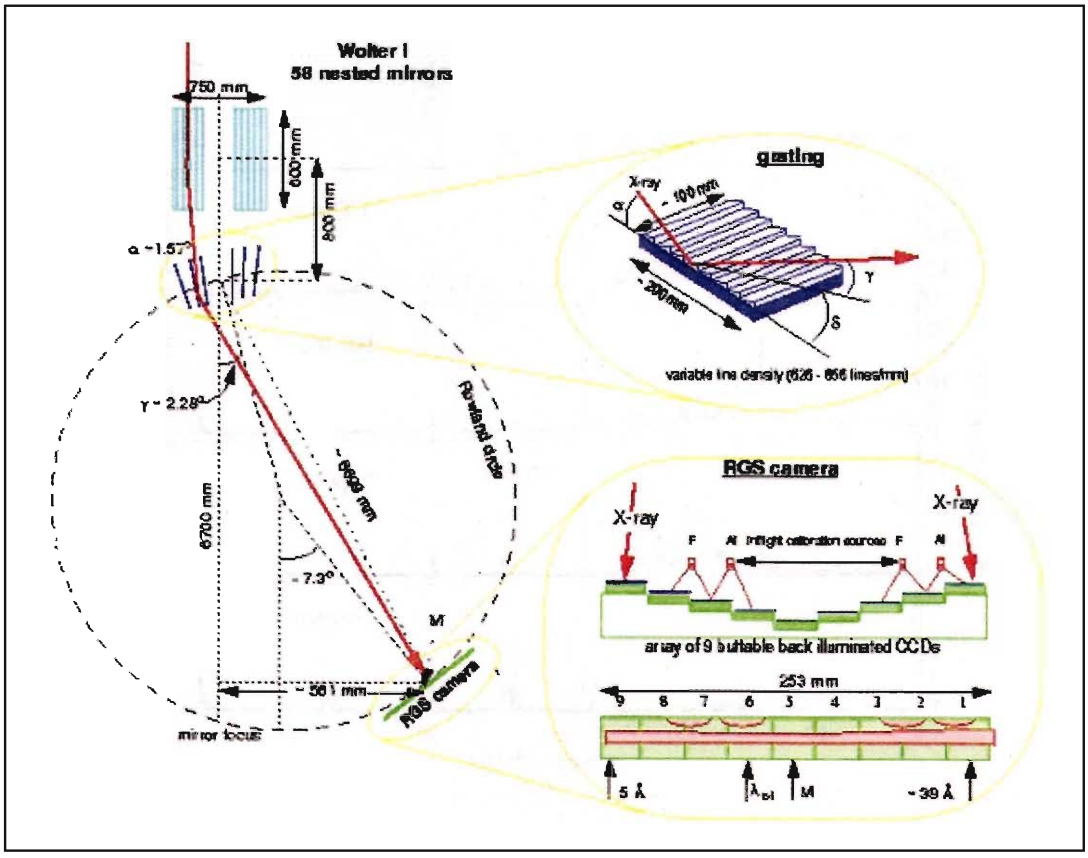

temperature in the range of 10-30 MK; (c) Capella, a late type giant star with a maximum temperature of 7 MK; and (d) Procyon, an F5 IV-V star with a maximum temperature of only 1-2 MK, like in our Sun. The hotter stars are also more luminous in X-rays and the differences in the line emission due to different coronal temperatures can be seen clearly in *Figure* 6. The line emission can provide a detailed diagnostics – density, temperature, composition, state of equilibrium of the hot plasma emission from stars and other X-ray sources (clusters of galaxies and supernova remnants) containing hot ionized gas.

An example of transmission gratings is the High Energy Transmission Grating Spectrometer (HETGS) flying on *CXO* (*Figure* 7). The gold bars constituting the gratings are supported by a thin plastic membrane having thickness of a soap bubble

Figure 5. A schematic of the Reflection Grating Spectrometer flying on XMM-Newton. The grating array has 182 gold-coated Silicon Carbide (SiC) plates, each with finely-ruled grooves on their surface. The gratings are housed in a Beryllium support structure positioned where light exits the mirror module. The dispersed light is recorded by a camera containing a row of 9 CCD detectors sensitive to the soft X-rays from 5Å to 35Å.

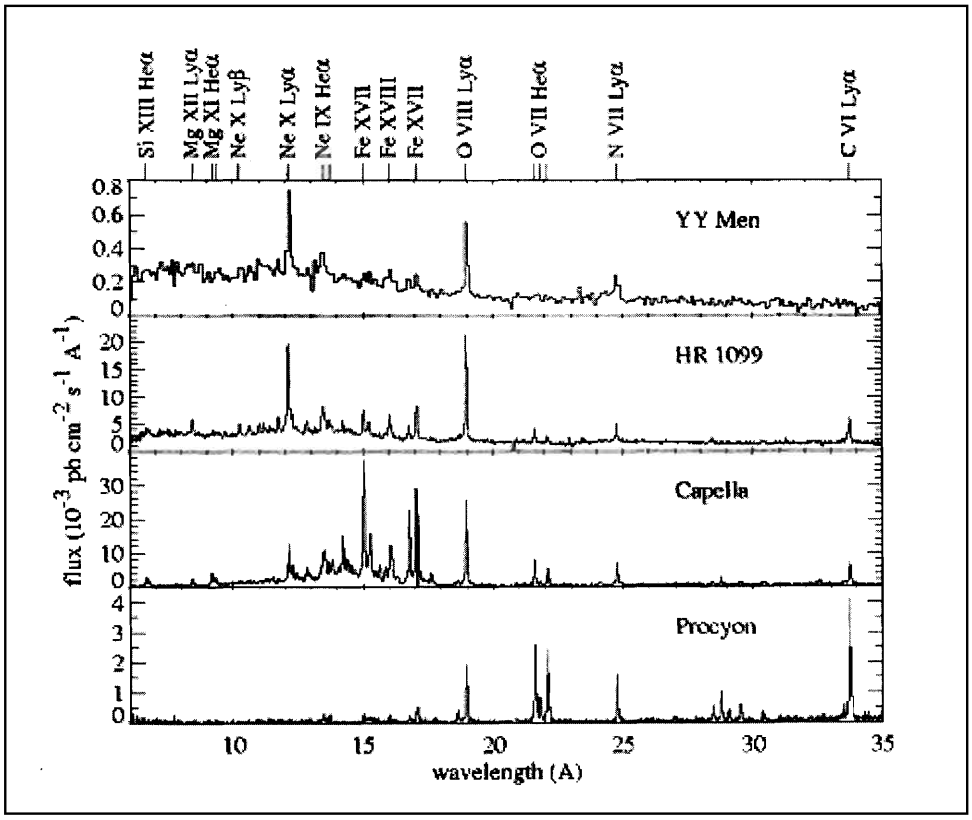

Figure 6. Examples of high-resolution X-ray spectrum of active stars taken with the Reflection Grating Spectrometer onboard XMM-Newton. Lines identified with various ionic transitions are marked.

(*Figure* 7 lower right), yet able to withstand launch shock and vibrations. The gratings take advantage of the fact that the gold bars are partially transparent to X-rays, so that the diffraction is more efficient, and more X-rays are captured in the high-resolution spectrum. The X-rays are dispersed into two intersecting lines corresponding to the MEG and the HEG with un-dispersed zero-order image in the centre and positive and negative orders on its opposite sides. The dispersed X-rays are captured by an array of CCDs. Spectra are constructed by summing the photons in different orders.

A spectrum taken with the transmission gratings on *Chandra* is shown in *Figure* 8. In this spectrum of an extremely powerful nucleus of a galaxy known as NGC 3783, specific elements (oxygen, neon, magnesium, silicon, sulfur, argon, and iron) around the nucleus – presumably due to a wind, reveal their

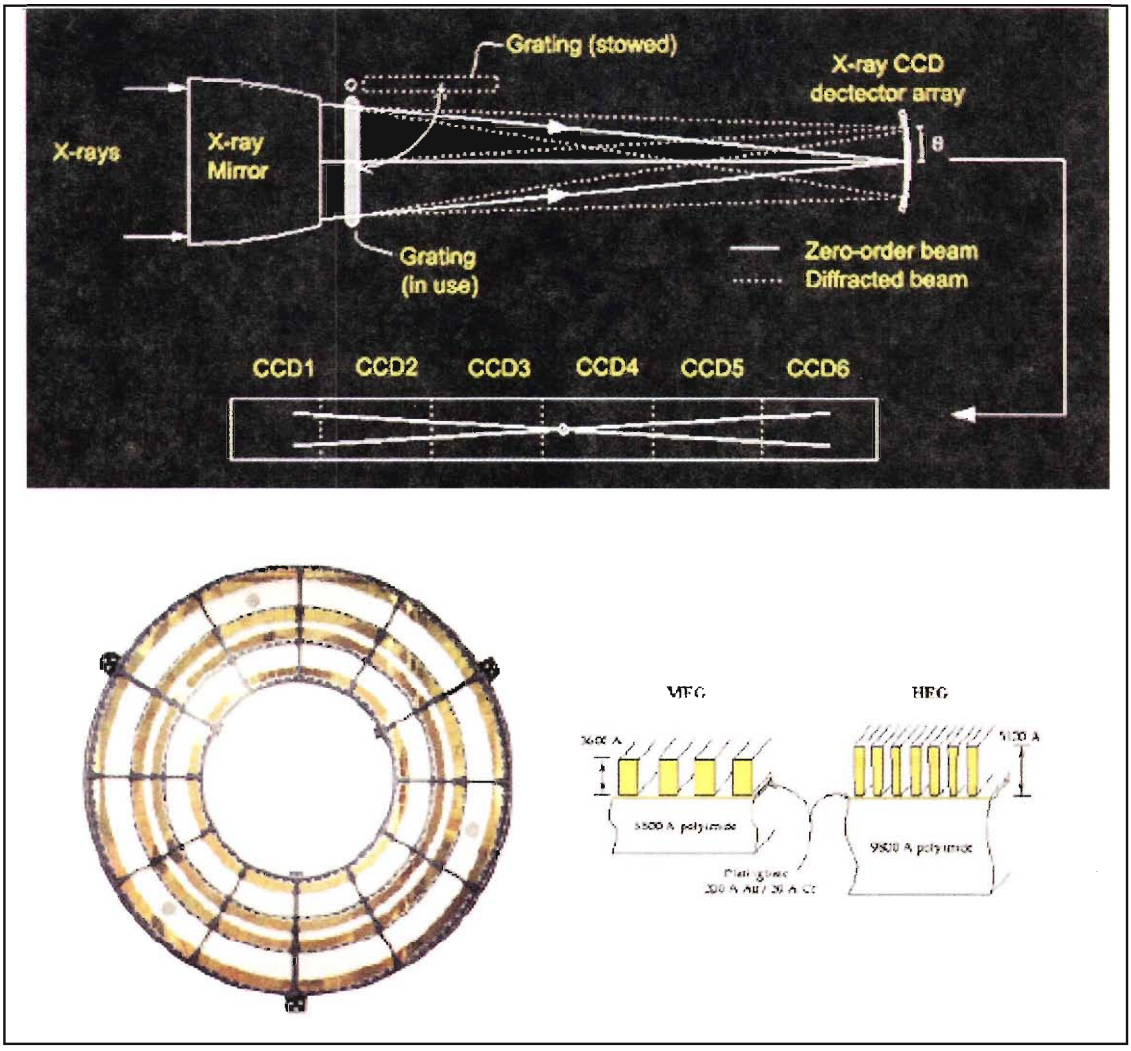

Figure 7. Medium and High Energy Transmission gratings onboard the Chandra X-ray Observatory. It consists of 336 gold bars mounted on an assembly that can be swung into position behind the Chandra mirrors. The bars (lower right) are regularly spaced by 0.2μm or 2000Å for the high-energy gratings, and 0.4μm or 4000Å for the medium energy gratings. The mounting of the facets (lower left) and the details of the facets (lower right) are shown. The inner two rings (lower left) are for the high-energy grating, HEG facets, and the outer two rings are medium-energy grating, MEG, facets. These gratings extend to a much higher energy range (1.5 Å or 8 keV) than the RGS in XMM-Newton.

presence by sharp absorption dips marked in the plot. The widths and locations of these dips tell us about the velocities in the extreme environment of the galaxy's core. Based on this spectrum, it is surmised that the intense radiation produced by

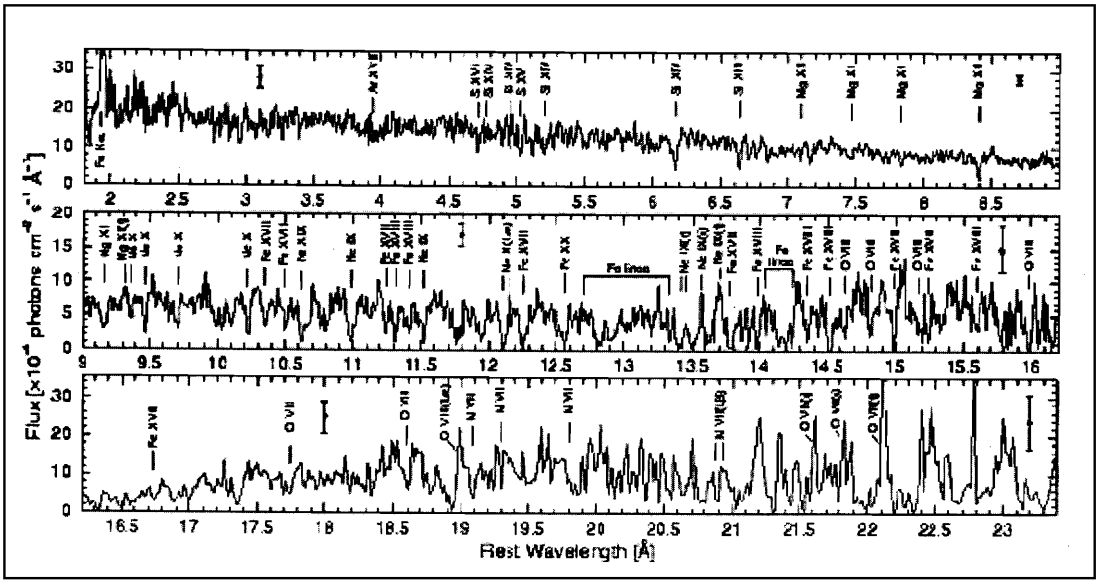

Figure 8. High resolution X-ray spectrum of the active nucleus in a galaxy, NGC 3783, taken with Chandra's Medium and High Energy Transmission gratings.

matter before it plunges into the black hole, heats the surrounding gas and drives a million km per hour wind away from the central black-hole.

Suggested Reading

[1] G W Fraser, *X-ray Detectors in Astronomy*, Cambridge University Press, Cambridge, UK, 1989.

[2] http://chandra.harvard.edu/ for more on Chandra X-ray Observatory and the latest results from CXO.

[3] http://heasarc.gsfc.nasa.gov/ for details and links to all the X-ray observatories flown so far or being planned.

[4] http://sci.esa.int/science-e/www/area/index.cfm?fareaid=23 for more on the XMM-Newton and the latest results from XMM.

The above references and sites are credited for the pictures and figures included here.

Address for Correspondence
Kulinder Pal Singh
Department of Astronomy and Astrophysics
Tata Institute of Fundamental Research
Homi Bhabha Road
Mumbai 400 005, India.
Email:singh@tifr.res.in